3GPP NB-IoT coverage extension using LEO satellites

Sylvain Cluzel, Laurent Franck, José Radzik, Sonia Cazalens, Mathieu Dervin, Cédric Baudoin, Daniela Dragomirescu

3GPP NB-IoT coverage extension using LEO satellites

Sylvain Cluzel *‡, Laurent Franck †, José Radzik ‡, Sonia Cazalens §,
Mathieu Dervin ¶, Cédric Baudoin ¶ and Daniela Dragomirescu ‖
* Laboratoire TéSA, Toulouse (France) – sylvain.cluzel@tesa.prd.fr
†IMT Atlantique, site de Toulouse ‡ISAE-Supaéro, Toulouse – jose.radzik@isae.fr
§Centre National d'Études Spatiales, Toulouse – sonia.cazalens@cnes.fr
¶Thales Alenia Space, Toulouse {cedric, mathieu}.{baudoin, dervin}@thalesaleniaspace.com
‖INSA-LAAS/CNRS, Toulouse – daniela@laas.fr

***Abstract*—Machine-Type Communications are meeting a growing interest on the consumer market. Dedicated technologies arise to support more robust communications involving a massive number of low cost, low energy-consuming devices This paper discusses the coverage extension of a Low-Powered Wide Area Network using a Low Earth Orbit satellite constellation, benefiting from the improved performance of a recent standard. The transmission complies with the user equipment specifications standardized as NB-IoT by 3GPP in Release 13. This radio technology is an update on LTE standard with enhanced performances: the supported path loss can be 20 dB higher than with legacy LTE. This improvement makes satellite-compatible the small and energy-constrained devices. A specific unidirectional system is defined, and a link budget is derived. Also, a receiver architecture is presented, that takes into consideration satellite channel specific impairments.**

I. Introduction

The Internet of Things (IoT) relates to all technologies related to the automated communications between any devices [1], such as control or sensing. Machine-to-Machine (M2M) communications ensure these devices are able to connect and communicate together in a specific network.

M2M market is expected to grow in the forthcoming years. The networks are now designed to handle a massive number of devices. This trend, motivated by industrial needs, will lead to the possibility of interconnection of more and more devices together, on different scales. Wireless networking is one of the growing topics related to IoT.

Low Power Wide Area Networks (LPWAN) are dedicated to connect devices with very specific constraints. The transmission can be long-range (over 10 km), while the device autonomy is typically about 10 years with two AA batteries, constraining the power consumption. Moreover, the system sizing usually relies on sparse resource allocation to the users, so as to handle a massive number of connected devices: several hours, or days, can be allowed between successive messages, the data rate being usually very low, typically below 500 bps. Non-critical data communications are not driven by the transmission delay, which can reach up to a few hours.

Several technologies are emerging to support such transmissions [2]. On the one hand, narrowband technologies use small bandwidth (less than 25 kHz, down to 100 Hz) to improve the link budget. On the other hand, spread spectrum technologies are well suited to manage intra-system interference.

Terrestrial networks involve costly ground infrastructure deployment, leading the service providers to focus on the most populated areas.

The use of satellites is an attractive option to extend LPWAN service coverage, and all the more if it does not imply specific user terminals. In [3], the authors study a M2M satellite system using ultra narrowband.

In this paper, we explore the opportunity to address 3GPP LTE NB-IoT compatible devices [4], [5], in a satellite network based on a Low Earth Orbit (LEO) constellation. In terrestrial NB-IoT, the medium access is controlled by the eNB (evolved Node B), which ensures that transmissions are not interfered through a combination of supervised timing synchronization and orthogonal channel allocation. In the proposed system, the user terminals are operated regardless of the space segment. We consider a unidirectional return link from the terminal to the satellite. There is no clock synchronization between the devices and the satellites. The devices transmit the data on a specific carrier, but on a randomly chosen subcarrier. In the proposed architecture, the satellites continuously and transparently digitize the received signal.

In absence of synchronization and scheduling, the received signal at satellite input will be impaired by intra-system interference. On the one hand, the high speed motion of LEO satellites induce a Doppler shift, resulting in inter-carrier interference. On the other hand, signal collisions will occur in this unscheduled transmission scheme. A similar two-dimension interfering scheme has already been studied for Time-Frequency Aloha [6]. In is shown in [7] that thanks to forward error correction (FEC), a high global system throughput may still be reached in such interfered system.

With no FEC, the expected throughput is low. But it is known that adding a FEC on the receiver side leads to a better global performance. NB-IoT standard allows the use of both turbocode spreading and repetition code spreading. Using a code makes the transmission more robust to interference. The performance improvement with a simple coding scheme has been assessed in [8]. However, to the authors' knowledge, the performance of a repetition code spreading under a Time-Frequency Aloha interference scheme has not been studied yet. Repetitions are being used for a coherent summation, calling for a specific demodulation model.

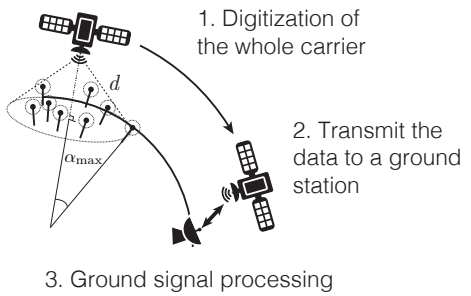

Fig. 1: Illustration of the system

Thus, in order to improve the demodulation of these possibly highly interfered transmissions, a Successive Interference Cancellation (SIC) technique is used. In order to ease the satellite payload complexity, the digitized signal is assumed to be processed at the ground station.

Intra-system interference penalty is all the more impacting as the channel load grows. In this paper, we focus on the performance of a single end-to-end satellite link. The intra-system interference cancellation is not addressed at this stage where the study purpose is to assess the satellite link feasibility and the related demodulation performance. Future work will address global throughput assessments for highly loaded systems, involving interference management.

The system model is presented in section II. A brief presentation of NB-IoT and a link budget is proposed. In section III, we define the performance metric and the load of such a system. Then, we propose a signal processing strategy that takes into account the satellite channel in section IV. Our algorithm is evaluated without interference in section V, in order to derive the link performance in terms of packet error rate (PER). In section VI, we draw some concluding remarks and propose some future work.

II. System overview

A. System presentation

A store and forward satellite system based on a LEO constellation is considered in this study, as illustrated on Figure 1. Satellites are used to digitize, and store the whole user bandwidth. Then, the data is transmitted to dedicated stations using a specific high throughput link. The satellite payload could be dedicated to the system, or hosted by an other constellation. In the ground station, the received signal is processed to extract the user messages from the aggregated signal. For this study, we consider that the satellite component allows to extend the terrestrial NB-IoT system, based on a dedicated bandwidth. The terminals are assumed to target the satellite system as soon as they are out of the terrestrial system coverage. The terminals transmit the data to the satellite in line of sight, in a dedicated bandwidth, but over a random subcarrier, without any previous time synchronization or coordination. No information on the user terminal locations is available in the satellite system. At the ground station level, the received signal is processed without a priori knowledge on the precise frequency, or packet time of arrival. Under these assumptions, to simplify the detection and the demodulation, we consider the same waveform parameters for all the terminals. More specifically, the modulation order, code rate, and message duration are identical for all terminals. As LEO satellite communications are considered, Doppler shift and rate must be taken into consideration in the transmission channel modeling. On the one hand, the received signal frequency localization bandwidth is extended in the Doppler shift range induced by the satellite move. On the other hand, the received signals are possibly impacted by nonnegligible Doppler drift rates, i.e. the time varying Doppler shift, with a subsequent degradation of the detection performance.

TABLE I: Some satellite parameters used by our system

Uplink central frequency, f_0	950 MHz
Satellite altitude	800 km
Satellite G/T	-24.1 dBK^{-1}
Satellite antenna HPBW[1]	120°
Equivalent minimal elevation	12.9°
Equivalent beam coverage radius	1900 km

[2]HPBW = Half Power Beam Width.

The studied system is characterized in Table I.

B. NB-IoT description

For this study, all transmissions are assumed to be based on NarrowBand-IoT (NB-IoT) air interface. Since June 2013, M2M communications are targeted by 3GPP. New releases have been published to progressively support low-cost, low-powered devices, making the choice of using narrowband communications.

In August 2016, the LTE release 13 has been updated to handle a new category of terminal, providing low-cost, high autonomy devices, under the name of NB-IoT, with an improved coverage, allowing the devices to support a 20 dB-higher path loss than legacy LTE for low throughput terminals. This improvement is especially due to the possibility of using a smaller bandwidth, down to one single subcarrier transmission (3.75 or 15 kHz). If the 3.75 kHz subcarrier is used, then the symbol rate is four times lower than LTE as defined by former releases. In this paper, we consider only the narrowest available subcarrier size. The modulation order, the transport block size index I_{TBS}, the resource units index I_{RU} and the number of repetitions are fixed for every terminal The waveform settings considered in this study are summarized in Table II. The frame structure is illustrated in Figure 2.

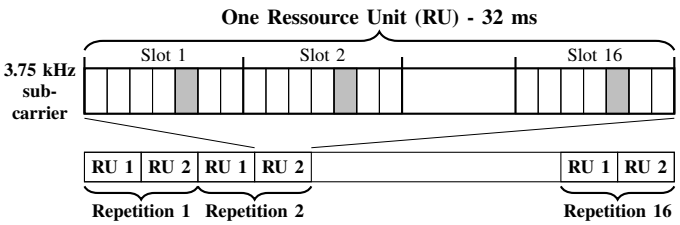

Fig. 2: Reference NB-IoT frame format. Pilot symbols are indicated in gray.

TABLE II: Reference NB-IoT waveform parameters

Emitted power	23 dBm
Bandwidth, BW	180 kHz
Subcarrier	3.75 kHz
Modulation	QPSK
Modulation format	single-tone SC-FDMA
Pilot symbol spreading	one every 7 symbols
Coding scheme	3GPP 1/3-Turbo code
Number of repetitions	16
I_{TBS}[1]	3
I_{RU}[1]	1

[1]These parameters, extracted from [5], design the transmissions. These values represent a transmission using QPSK, containing 104 bits payload, and of duration 1.024 s. Note that there is no delay between repetitions.

C. Link budget

In this paragraph, we aim to express the distribution of SNR, and Doppler drift rate of the transmissions. The SNR distribution, denoted f_{SNR}, is derived analytically, and the Doppler rate is obtained by simulations. We model the satellite channel from the terminal to the satellite with an additive white Gaussian noise. Receiver signal to noise ratio (SNR) notably depends on the relative position of the terminal and the satellite. The parameter α refers to the angle between a fixed terminal position and the satellite nadir, and d to the distance between the terminal and the satellite, as represented in Figure 1. Let's α_{max} be the maximum value taken by α, i.e. when a terminal is at the edge of coverage, and the elevation is minimal. Then, denoting k_B the Boltzmann constant, and L_{other} the other losses than the free space losses [9]:

$$\text{SNR}(\alpha) = \frac{\text{EIRP} \cdot (G/T)}{k_B \cdot \text{BW} \cdot \left(\frac{4\pi f_0}{c}\right)^2 \cdot L_{\text{other}} \cdot d^2} \tag{1}$$

We suppose that the user location probability is uniform in the satellite coverage. We use d_u, the user spatial density per km with relation to α, defined as:

$$d_u(\alpha) = \frac{\sin(\alpha)}{(1 - \cos(\alpha_{\text{max}}))} \tag{2}$$

$$f_{\text{SNR}}(x) = \frac{1}{\text{SNR}'(\text{SNR}^{-1}(x))} d_u(\text{SNR}^{-1}(x)) \tag{3}$$

We use the formula of change of variable in the probability function, recalled in (3), to obtain f_{SNR} represented in Figure 3a. The lower received signal-to-noise ratio (i.e. when the terminals are the edge of coverage) is around -5 dB.

In [10], SNR values about -12 dB leads to a block error rate lower than 10%. On Figure 3a, we can see that the worst SNR met in the proposed system is higher than the one supported by terrestrial NB-IoT. Although this is not evaluated here, it can be inferred that this margin is likely to be useful in case of intra-system interference.

Figure 3b displays the probability density function of the Doppler drift rate, obtained by simulations.

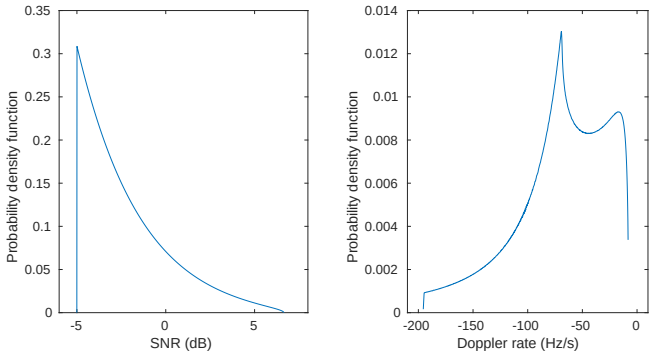

(a) SNR PDF (b) Doppler drift rate PDF

Fig. 3: SNR (3a) and a Doppler rate (3b) distribution for a 3.75 kHz subcarrier.

III. System metrics

The channel load is defined as the average number of simultaneously transmitting terminals, divided by the number of subcarriers. Due to Doppler spread, the signal bandwidth is widened at the satellite input with a favorable impact over the interference issue. We modify the load in relation to this spreading. The maximum frequency shift, with relation to our system, is:

$$\delta_{f,\text{max}} = f_0 \cdot V_{\text{sat,max}}/c \approx 23 \text{ kHz} \tag{4}$$

where c refers to the speed of light, and $V_{\text{sat,max}}$ the satellite speed that implies the most Doppler shift. Since the Doppler shift range is significantly larger than the subcarrier width, we consider a uniform spectral distribution of the received carriers at satellite level. At satellite input, the aggregated received signal bandwidth is extended to $\text{BW}_{\text{sat}} = 2\delta_{f,\text{max}} + \text{BW} = 226$ kHz. If the terminal spatial density and the message transmission rate are known, we define the channel load at satellite level $\rho_{\text{sat}} = \rho_g \cdot \text{BW}/\text{BW}_{\text{sat}}$, as a function of the system load ρ_g.

The proposed figure of merit to assess the system performance is the satellite load that will ensure a PER of 10^{-1}. In this paper, we only study interference free transmissions. This assumption is applicable to light load scenarios.

The channel load depends on the number of terminals, and the message transmission rate. The satellite cover area is $S_{\text{sat}} = \pi(\alpha_{\text{max}} R_{\text{earth}})^2$, with R_{earth} the Earth radius. Then, with the terminal density d_t, expressed in km^{-2}, the number of terminals in the satellite coverage is $N_t = d_t S_{\text{sat}}$. Every terminal is using the satellite system. If the devices transmit N_{m} messages per day, each message lasting T_{message} in seconds, the channel occupation ratio τ of one terminal is:

$$\tau = \frac{N_{\text{m}} \cdot T_{\text{message}}}{3600 \cdot 24} \tag{5}$$

The average number of simultaneously transmitting terminals under the satellite coverage is $\lambda_{\text{n}} = \tau N_t$, randomly spread over 48 subcarriers. The system load is then $\rho_g = \lambda_{\text{n}}/48$.

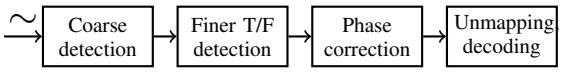

Fig. 4: Block diagram of the proposed synchronization strategy

With the previously chosen parameters, $d_t = 0.05$ km^{-2} (approximately half a million terminals in the satellite coverage), and $N_{\text{m}} = 1$, the satellite load is $\rho_{\text{sat}} = 0.11$. For this set of parameters, the channel load is considered as low. With this channel load, most of the transmissions do not undergo intra-system interference.

IV. Ground signal processing

A. Receiver description

In the studied system, the satellite digitizes and stores the received data, which are then transferred to dedicated ground stations. The detection and demodulation of the received transmissions are performed in the ground station. The receiver has no specific information on those transmissions, especially about the Doppler-shifted central frequency, the Doppler rate, or the message time of arrival. As the pilot sequence is known, the receiver will perform a data-aided detection and demodulation.

For the synchronization, a classical approach [11] has been developed, and is presented in Figure 4.

First, a coarse time and frequency domain signal detection is performed to have an approximation of the packet time of arrival and the central frequency of the received signal, based on a power detector. This step relies on a short-time Fourier transform. Note that this step could be omitted; consequently the next step would have to be parallelized to detect transmissions over the whole bandwidth; a massive computation power would be needed.

Then, a finer time-frequency detection is performed using a filter-bank. As detailed in the next section, in order to compensate for the possibly significant Doppler rate impact over the message duration (see Figure 3b), the frequency is separately estimated at the beginning and at the end of the packet.

Then, a phase correction is performed by solving an optimization problem, as described in [12].

Finally, a classical demodulation method is implemented. A power and SNR estimation is performed on the synchronized signal. Using this information, we compute the log-likelihood ratio (LLR) of each symbol. These LLR are summed over each repetition, as proposed in [13] to optimize the decoding performance. The result of the summation is provided to the turbodecoder.

B. Presentation of our detection method

The receiver should be able to detect a 3.75 kHz transmission within 226 kHz wide sampled signal. We first compute a 2D-power detection, using a short-time Fourier transform (STFT). In our implementation, the STFT resolution is similar in the time and in the frequency domain, to represent the transmission with as many STFT samples as possible. Then,

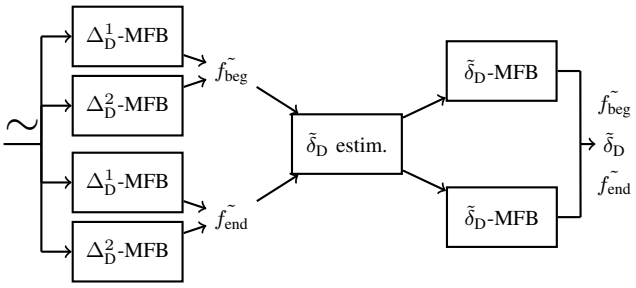

Fig. 5: Block diagram of the detection method, for $n_d = 2$

a 2D-cross-correlation is performed between the computed STFT and the STFT of a theoretical transmission, in order to obtain a coarse estimation of the time of arrival, and of the related central frequency, despite the high range of frequency rate. The residual frequency error can be up to 200 Hz, and the residual time error up to 50 ms for very low SNR.

Then, a classical fine frequency and time estimation structure is considered, using banks of Wiener filter (FB), as described in [11]. Each filter is a frequency-shifted cross-correlation between the pilot symbol sequence, and the received signal. The global maximum of the cross-correlation values gives an estimated time and frequency of the transmission. The number of required filters is deduced from the residual error after coarse detection, and from the frequency resolution of the filter bank.

As displayed in Table II, the duration of the transmission is approx. 1 s; in order to cope with possibly high Doppler rate (up to 200 Hz/s), the cross-correlation is split into two shorter parts. We perform each cross-correlation over N_{p} pilot symbols. The first and last symbols are respectively used to estimate the carrier frequency at the beginning and at the end of the packet. The value of N_{p} has been heuristically set to $N_{\text{p}} = 150$, that being approximately one third of the pilot symbol sequence.

To improve the detection performance in presence of Doppler rate, the filter banks are modified to include a frequency drift over the cross-correlation duration. In this purpose, the reference pilot sequence is multiplied by a quadratic complex chirp. The chirp frequency drift rate is denoted as Δ_{D}, and the MFB is mentioned Δ_{D}-MFB. If the difference between the chirp rate and the signal rate is too significant, the pilot sequence is not detected. So, to counterbalance the high range of Doppler rate, n_d values of Δ_{D} are used, so that the difference between Δ_{D} and the effective frequency rate of the transmission is minimized. Once the beginning and ending frequencies, f_{beg} and f_{end}, are estimated by the MFB with the highest likelihood, we obtain an approximation of transmission's frequency rate δ_{D}. This approximation is noted $\tilde{\delta}_{\text{D}}$. Then we use the MFB a second time, using $\Delta_{\text{D}} = \tilde{\delta}_{\text{D}}$ to estimate the f_{beg} and f_{end} with less error. This finer detection is represented in Figure 5 for $n_d = 2$.

The frequency estimation at the beginning and at the end of the packet must be very accurate to ensure the packet demodulation. In our simulation scenarios, the residual error

is found inferior to 10 Hz.

A joint phase and frequency estimation is finally performed as described in [12], by minimizing the mean square error between the known pilot sequence and the received data multiplied by a chirp, the parameters of which are estimated to fit the residual error after coarse and fine frequency detection.

V. Simulation results and analysis

This section is dedicated to the performance assessment of the proposed receiver in absence of interference.

A NB-IoT standard compliant signal is generated on a random subcarrier. The transmission is affected by the channel, especially by the Doppler effect. For this transmission, we perform the detection, the synchronization, and then the demodulation.

If the receiver manages to detect the transmission and estimate its frequency parameters, we consider the synchronization as successful. In such case, the turbodecoder decodes the transmission and the Cyclic Redundancy Check (CRC) returns no error. However, if the receiver does not estimate the transmission parameters with enough accuracy, the synchronization is a failure: the CRC detects an error, and the packet is lost. As the turbo-decoder would guarantee quasi-error free transmissions over an AWGN channel in this SNR range, all packet losses in our simulations can be imputed to the detection or to the synchronization.

In Figure 6, we compare the performance of our detection method to a reference case, without any frequency drift, using unmodified FB (dashed blue curve). These filters are designed to estimate the frequency shift. Then, we introduce the Doppler drift, without changing the method (crossed red curve). We can see that the Doppler drift degrades the performance. This is due to the nondetection of the transmissions that are affected by a high frequency drift rate, by the unmodified FB.

We present the performance of the MFB, using first $n_d = 1$ in yellow; the PER is lower, as expected. So the modifications of the filter bank imply a better resilience to the frequency drift. Increasing the value of n_d decreases the PER. Then, $n_d = 2$ and $n_d = 3$ are tested, and the performances are close to the case without frequency drift.

The very low PLR transmissions have a negligible impact on the system performance, which is mainly affected by the noisiest signals. A mean PER is estimated for the system, as a weighted average of SNR-specific PER estimations, using the SNR distribution illustrated. in Figure 3.

With this set of parameters, the system PER is found close to 3 %. As a conclusion, the goal of PER$< 10^{-1}$ is reached for very low loads.

VI. Conclusions

In this paper we describe a new system, designed to extend 3GPP NB-IoT terrestrial coverage to worldwide, using a constellation of LEO satellites. Our system is based on a unidirectional and unsynchronized link from the terminals to the satellite. Each satellite of the constellation digitizes and stores the targeted spectrum until it can be forwarded

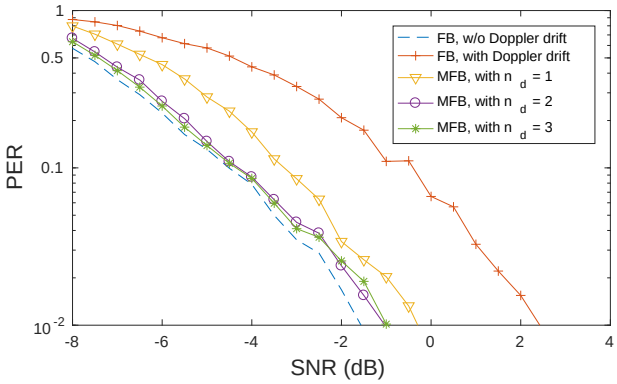

Fig. 6: Performance of different detection methods.

to a ground station, where the detection and demodulation is processed by the receiver. We derive an equivalent load for our satellite system, and we estimate an addressable number of terminals in the satellite coverage. The proposed detection algorithm is designed to minimize the impact of the satellite channel and more particularly the Doppler drift, in the demodulation performance. The global performance of our system is assessed under the assumption of low channel load.

Future research work will focus on the impact of intra-system interference to extend the study towards high load channel scenarios.

References

[1] *Recommendation ITU-T Y.4000/Y.2060*, ITU Std., June 2012.

[2] U. Raza, P. Kulkarni, and M. Sooriyabandara, "Low power wide area networks: An overview," *IEEE Communications Surveys Tutorials*, vol. 19, no. 2, pp. 855–873, Secondquarter 2017.

[3] M. Anteur, V. Deslandes, N. Thomas, and A. L. Beylot, "Modeling and performance analysis of ultra narrow band system for M2M," in *2016 8th Advanced Satellite Multimedia Systems Conference and the 14th Signal Processing for Space Communications Workshop (ASMS/SPSC)*, Sept 2016, pp. 1–6.

[4] *3GPP TS 36.211, LTE; Physical channels and modulation, v.14.3.0*, 3GPP Std., August 2017.

[5] *3GPP TS 36.212, LTE; Multiplexing and channel coding v.14.4.0*, 3GPP Std., October 2017.

[6] C. Goursaud and Y. Mo, "Random unslotted time-frequency ALOHA: Theory and application to IoT UNB networks," in *2016 23rd International Conference on Telecommunications (ICT)*, May 2016, pp. 1–5.

[7] V. Almonacid and L. Franck, "Throughput performance of time- and frequency-asynchronous ALOHA," in *SCC 2017; 11th International ITG Conference on Systems, Communications and Coding*, Feb 2017, pp. 1–6.

[8] ——, "An asynchronous high-throughput random access protocol for low power wide area networks," in *2017 IEEE International Conference on Communications (ICC)*, May 2017, pp. 1–6.

[9] G. Maral, M. Bousquet, and Z. Sun, *Satellite communications systems: systems, techniques and technology*, ser. Wiley Series in Communication and Distributed Systems. Wiley, 2009.

[10] A. Adhikary, X. Lin, and Y. P. E. Wang, "Performance evaluation of NB-IoT coverage," in *2016 IEEE 84th Vehicular Technology Conference (VTC-Fall)*, Sept 2016, pp. 1–5.

[11] U. Mengali, *Synchronization techniques for digital receivers*. Springer US, 1997.

[12] M. Morelli, "Doppler-rate estimation for burst digital transmission," *IEEE Transactions on Communications*, vol. 50, no. 5, pp. 707–710, May 2002.

[13] T. Sakai, K. Kobayashi, S. Kubota, M. Morikura, and S. Kato, "Soft-decision Viterbi decoding with diversity combining," in *Global Telecommunications Conference, 1990, and Exhibition. 'Communications: Connecting the Future', GLOBECOM '90., IEEE*, Dec 1990, pp. 1127–1131 vol.2.